RSC Advances

RSC Publishing

PAPER

View Article Online
View Journal | View Issue

Cite this: *RSC Advances*, 2013, **3**, 3414

Synthesis of nano-sized spherical Mg_3Al–CO_3 layered double hydroxide as a high-temperature CO_2 adsorbent

Qiang Wang,*[a] Yanshan Gao,[a] Jizhong Luo,[b] Ziyi Zhong,[b] Armando Borgna,[b] Zhanhu Guo[c] and Dermot O'Hare[d]

Received 23rd October 2012,
Accepted 19th December 2012

DOI: 10.1039/c2ra22607c

www.rsc.org/advances

Due to its layered structure, layered double hydroxides (LDHs) generally prefer to form either ''sand rose'' or platelet-like morphologies. To the best of our knowledge, nano-sized spherical LDHs have not been previously reported. In this work, we present the first successful synthesis of nano-sized spherical Mg_3Al–CO_3 LDH using a facile isoelectric point (IEP) method. SEM and TEM analyses confirmed that the size of the nanospheres is very uniform, with an average value of *ca.* 20 nm. Furthermore, a mesoporous LDH sample composed of the above synthesized uniform nano-spheres can be prepared, and this material showed a H1 type hysteresis loop in the N_2 BET analysis. Such mesoporous LDH possesses large mesopores (18 nm) and a high surface area (103 $m^2\ g^{-1}$), which we believe make it a promising adsorbent, catalyst, or support material. We demonstrated that its CO_2 capture capacity is 0.83 mmol g^{-1} at 200 °C and 1 atm and it can be further increased up to 1.21 mmol g^{-1} by doping with 20 wt% K_2CO_3.

1. Introduction

The sorption-enhanced water gas shift (SEWGS) process, which is a combination of the WGS reaction and CO_2 adsorption, has been widely identified as a promising pre-combustion CO_2 capture technology.[1–3] By adsorbing and removing CO_2 from the reaction mixture, the reaction is driven to the right-hand-side, thereby completely converting CO and maximizing the production of H_2. SEWGS produces a hot stream of hydrogen and steam, which can be directly fed to a gas turbine, and a cooled stream of pure CO_2, which can be compressed and transported for further storage and utilization. To ensure the success of this technology, it is crucial to have good CO_2 adsorption materials.[4–7] Among many different solid adsorbents, layered double hydroxides (LDHs) have been regarded as one of the most promising CO_2 adsorbents for the SEWGS process.[8–12]

LDHs $[M^{z+}_{1-x}M^{y+}_{x}(OH)_2]^{a+}(X^{n-})_{a/n}{\bullet}mH_2O$ (M^{z+}, z = 1 or 2; M^{y+}, y = 3 or 4) are a class of ionic lamellar compounds made up of positively charged brucite-like layers with an interlayer region containing charge compensating anions and solvation molecules.[13,14] Because the chemical composition of both the inorganic layers and the interlayer gallery anions can be precisely controlled, LDHs possess highly tuneable properties and can potentially be used in a wide range of applications such as high-temperature CO_2 capture,[8,9,15] catalysts,[16,17–19] ion exchange hosts,[20–22] fire retardant additives,[23,24] cement additives,[25] polymer–LDH nanocomposites,[26,27] drug delivery,[28] luminescent materials,[29,30] magnetic materials,[31,32] *etc.*

To date, many studies have been performed on LDH-derived CO_2 adsorbents; for instance, the effects of divalent cations,[33,34] trivalent cations,[9] charge compensating anions,[10,35] Mg–Al ratio,[36] synthesis method,[37] the presence of SO_2 and H_2O,[38,39] and particle size.[40] The main problem of this material is its insufficient CO_2 capture capacity. It is suggested that doping K_2CO_3 on LDHs significantly increases the CO_2 capture capacity.[41–43] However, one drawback is that doped K_2CO_3 might block the pores of the LDH derivatives and consequently lower its adsorption capacity.[44–47] In general, the reported CO_2 capture capacity is 0.5 mmol g^{-1} for pure LDH and 0.85 mmol g^{-1} for K_2CO_3–LDHs.[38,39,42,48,49] For similar reasons, solid amines, which are good low-temperature CO_2 adsorbents, are normally supported on the mesoporous substrates.[8] Therefore, in order to increase the CO_2 capture capacity of LDHs, one efficient way is to decrease the particle size, and another is to fabricate mesoporous type LDH samples that can lead to a better dispersion of doped K_2CO_3 species.

LDHs have been extensively synthesized and studied for decades. Currently, many synthesis approaches including co-precipitation,[50] urea hydrolysis,[51] structure reconstruction,[52] sol–gel,[53] ion exchange,[54] and reverse microemulsion[55] have been developed. In order to increase the crystalline degree or

[a]*College of Environmental Science and Engineering, Beijing Forestry University, 35 Qinghua East Road, Haidian District, Beijing, 100083, P. R. China. E-mail: qiang.wang.ox@gmail.com; qiangwang@bjfu.edu.cn; Tel: 86-13699130626*
[b]*Institute of Chemical and Engineering Sciences (ICES), A*STAR, 1 Pesek Road, Jurong Island, 627833, Singapore*
[c]*Dan F. Smith Department of Chemical Engineering, Lamar University, Beaumont, TX 77710, USA*
[d]*Department of Chemistry, University of Oxford, Mansfield Road, Oxford, OX1 3TA, United Kingdom*

to control the morphology of LDHs, the aging process can be further assisted by either hydrothermal treatment,[56] sonication,[57] or microwave irradiation.[58] However, due to the layered structural feature of LDH, it generally prefers to form either sand rose[59] or platelet-like[60] morphologies. To the best of our knowledge, spherical LDH, particularly on the nano-scale, has not yet been reported.

In this paper, we report a very facile method for the successful synthesis of nano-sized spherical Mg_3Al–CO_3 LDH, and the crystal formation was well explained by employing the isoelectric point (IEP) concept. Furthermore, by aggregating these nanoparticles, a unique mesoporous LDH composed of uniform nanospheres (*ca.* 20 nm on average) can be obtained. These LDHs have been characterized by X-ray diffraction (XRD), BET, scanning electron microscopy (SEM), transmission electron microscopy (TEM), and dynamic light scattering (DLS). Their performance as high-temperature CO_2 adsorbents was evaluated using thermogravimetric analysis (TGA).

2. Experimental

2.1 Synthesis of samples

Conventional coprecipitation method. In brief, a salt solution A (100 mL) containing a mixture of 0.075 mol $Mg(NO_3)_2{\cdot}6H_2O$ and 0.025 mol $Al(NO_3)_3{\cdot}9H_2O$ was added drop-wise to a basic solution B (100 mL) containing 0.05 mol Na_2CO_3. The pH value of solution B was kept constant at 10 by addition of a solution C (50 mL) containing 0.17 mol NaOH. The resulting mixture D was aged at room temperature for 24 h with continuous stirring. The aged mixture was filtered and washed with deionized water until pH = 7, followed by drying at 100 °C in an oven. The obtained LDHs are denoted as LDH (CC).

Synthesis of LDHs. The LDHs were synthesized *via* a method modified from the conventional coprecipitation method. Because the IEP of Mg_3Al–CO_3 is around 10,[61,62] a higher pH of 12 was deliberately used in order to make the surface of LDH primary particles negatively charged. The pH of the precipitation solution was kept constant at 12 by adding NaOH solution (3.4 M) drop-wise, and the whole synthesis process took 1 h. Under such basic conditions, the LDH formation rate was so fast that the growth along all directions was the same and spherical nanoparticles were formed. Due to the repulsive force between negatively charged LDH primary particles and $Al(OH)_4^-$, CO_3^{2-}, OH^- anions, its growth was inhibited, leading to the formation of nano-sized particles (*ca.* 20 nm). All other synthesis parameters were kept unchanged. Since the concept of IEP is used, the obtained LDHs are denoted as LDH (IEP).

Synthesis of K_2CO_3–LDH. For the synthesis of K_2CO_3–LDH, LDH was first pretreated at 400 °C in an Ar flow for 5 h. Then 2 g calcined LDH and 0.4 g K_2CO_3 was mixed in 50 mL aqueous solution and stirred at room temperature overnight. The water was then removed under reduced pressure. Finally, the obtained sample was dried at 100 °C for further study.

2.2 Characterization of LDH (CC) and LDH (IEP)

BET analysis. The BET specific surface areas were measured from the N_2 adsorption and desorption isotherms at 77 K collected using a Quantachrome Autosorb-6B surface area and pore size analyzer. Before each measurement, fresh HTs were first degassed at 110 °C overnight.

XRD analysis. Powder XRD analyses were conducted in a Bruker D8 Advance X-ray diffractometer equipped with a RINT 2000 wide-angle goniometer using Cu-Kα radiation and a power of 40 kV × 40 mA. Diffraction patterns were recorded within the range 2θ = 5–70° with a step size of 0.02°.

SEM analysis. The morphologies of synthesized LDHs were observed using SEM (JEOL JSM-6700F). Before observation, the dried samples were sputtered and coated with gold for ~120 s under an argon atmosphere.

TEM analysis. TEM measurements were conducted using a TECAI TF20 Super Twin (200 kV) electron microscope, whereby a drop of solution was placed onto a Cu grid and dried in air.

DLS analysis. The DLS diameter of LDHs was measured using photon correlation spectroscopy (PCS, Nanosizer Nano ZS, Malvern Instruments).

2.3 Evaluation of CO_2 capture capacity

The adsorption of CO_2 on LDHs was measured using a thermogravimetric method on a Q500 TGA analyzer. Samples were calcined at 400 °C for 5 h in an Ar atmosphere before CO_2 adsorption experiments. To minimize potential errors caused by the memory effect, all experiments were carried out immediately after the first calcination. CO_2 adsorption experiments were carried out at 200 °C and 1 atm with a constant flow of CO_2 (40 mL min^{-1}).

3. Results and discussion

3.1 Synthesis of LDHs

Although the IEP method has been frequently used in novel materials synthesis and design, its application in the synthesis of LDHs has not been previously reported.[63–65] Here we report the first synthesis of LDHs using the concept of an IEP method, from which special nanospherical morphology can be obtained. According to the IEP mechanism (see Fig. 1(a)), the net charge of the particles is affected by the pH of their surrounding environment. It can be positively (pH < IEP), neutrally (pH = IEP) or negatively (pH > IEP) charged depending on the relationship between the IEP and the pH.[66,67] In our preparation, a metal precursor solution containing $Mg(NO_3)_2$ and $Al(NO_3)_3$ was added drop-wise to the precipitation solution containing Na_2CO_3, and the pH of the precipitation solution was deliberately controlled at a constant value of 12 using NaOH solution during the whole process. The key point of this method is to finely control the pH value ($\geqslant$12) of the precipitation solution. The zeta potential of the Mg_3Al–CO_3 LDH was measured in different pH conditions, as shown in Fig. 2. At pHs of 8 and 12, its zeta potential is + 25 and −30 mV, respectively. This further confirms that the surface of the LDH is negatively charged when the synthesis pH is 12. Under such basic conditions, the

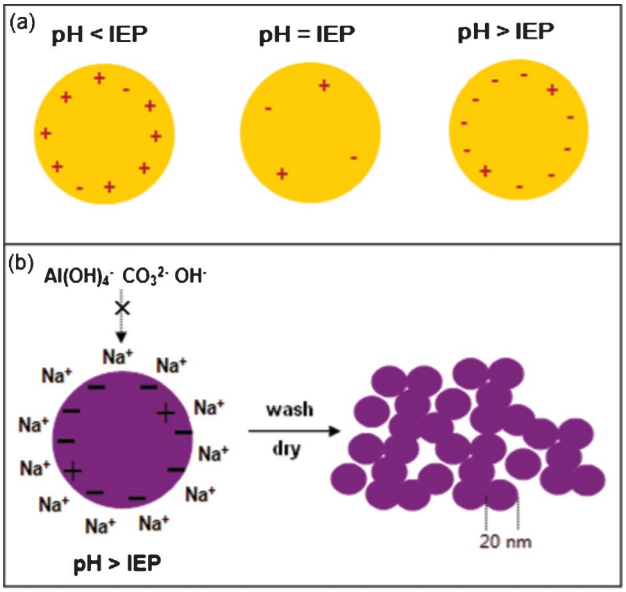

Fig. 1 (a) The relationship between surface charge and solution pH values. (b) The synthesis mechanism of nanospherical LDH by the method induced from the IEP concept.

rate of LDH formation is so fast that the growth in all directions is equal and so spherical nanoparticles form. Since the IEP of the Mg_3Al–CO_3 LDH is 10,[61,62] the surface of the primarily formed LDH nanoparticles (NPs) is negatively charged. Any further contacts between LDH NPs and anions like $Al(OH)_4^-$, CO_3^{2-}, and OH^- are not favoured, inhibiting the growth of the LDH particles. Therefore, using this synthesis method, uniform spherical Mg_3Al–CO_3 nanoparticles can be synthesized.

Furthermore, a unique mesoporous LDH sample composed of uniform LDH nanospheres could be obtained by the aggregation of the above nanoparticles (see Fig. 1(b)). For comparison, a LDH with a ''sand rose'' morphology was also synthesized by the conventional coprecipitation method. In

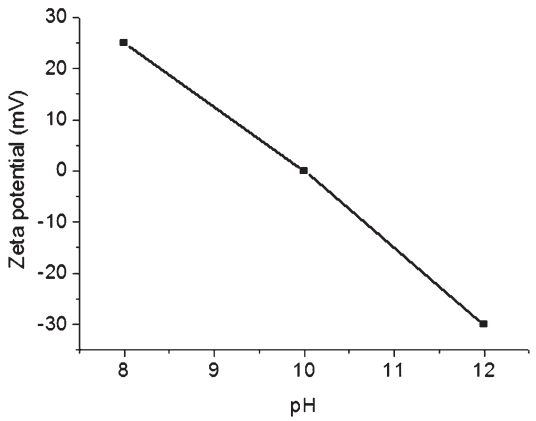

Fig. 2 The zeta potential of Mg_3Al–CO_3 LDH measured in different pH conditions.

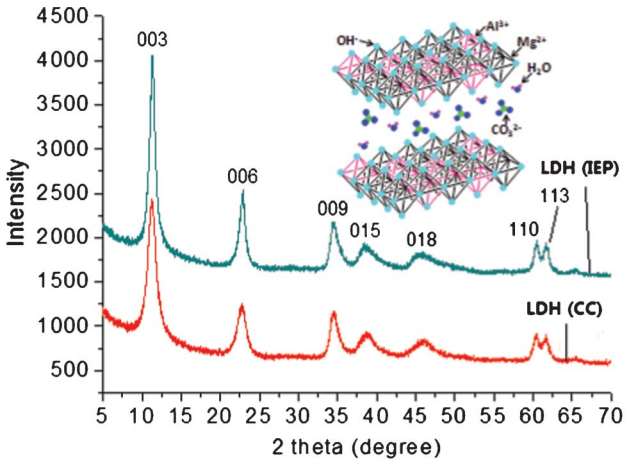

Fig. 3 XRD patterns of LDH (CC) and LDH (IEP). The inset shows the schematic structure of Mg_3Al–CO_3.

the following parts, both Mg_3Al–CO_3 (CC) and Mg_3Al–CO_3 (IEP) were carefully characterized and their CO_2 capture performances were evaluated.

3.2 Characterization of mesoporous LDH

Synthesized Mg_3Al–CO_3 LDHs were first characterized by XRD, as shown in Fig. 3. It is apparent that both LDH (CC) and LDH (IEP) have formed a typical layered double hydroxide structure. All the characteristic Bragg reflections for a LDH were observed for both samples. The interlayer distance (d_{003}) was *ca.* 7.80 Å. The reflections between 60 and 65°, which correspond to a unit cell of a = *ca.* 3.1 Å, suggest that the Al^{3+} cations are randomly distributed (disordered) within the layers.[68] We see no evidence for any difference in their crystal structures. The inset of Fig. 3 shows the schematic structure of Mg_3Al–CO_3.

The pore size and pore shape were analyzed from the N_2 adsorption and desorption isotherms at 77 K collected using a Quantachrome Autosorb-6B surface area and pore size analyzer. Before each measurement, fresh LDHs were first degassed at 110 °C overnight. LDH (IEP) shows a H1 type hysteresis loop, indicating that the pores are produced by the aggregation of uniform spheres (Fig. 4(a)). The inset of Fig. 4(a) shows an average pore size of *ca.* 18 nm. However, LDH (CC) shows a H3 type hysteresis loop, suggesting that the pores are produced by the aggregation of plate-like particles (Fig. 4(b)).[69] The inset of Fig. 4(b) shows the typical pore size distribution of LDH (CC). Two peaks were observed at 3.7 and 6.3 nm, both of which are much smaller than that of LDH (IEP).[9] The specific surface areas of LDH (IEP) and LDH (CC) are 103 and 114 $m^2\ g^{-1}$, respectively.

The BET results were confirmed by SEM and TEM analyses, as shown in Fig. 5 and 6. LDH (CC) exhibited a spheroidal ''sand rose'' morphology. The size of the ''flower ball'' is approximately 400–450 nm, and the thickness of the petals is about 24–25 nm, accounting for about 30–32 brucite-like sheets. LDH (IEP) contained aggregates of uniform nanospheres with an average size of *ca.* 20 nm. The formation of the

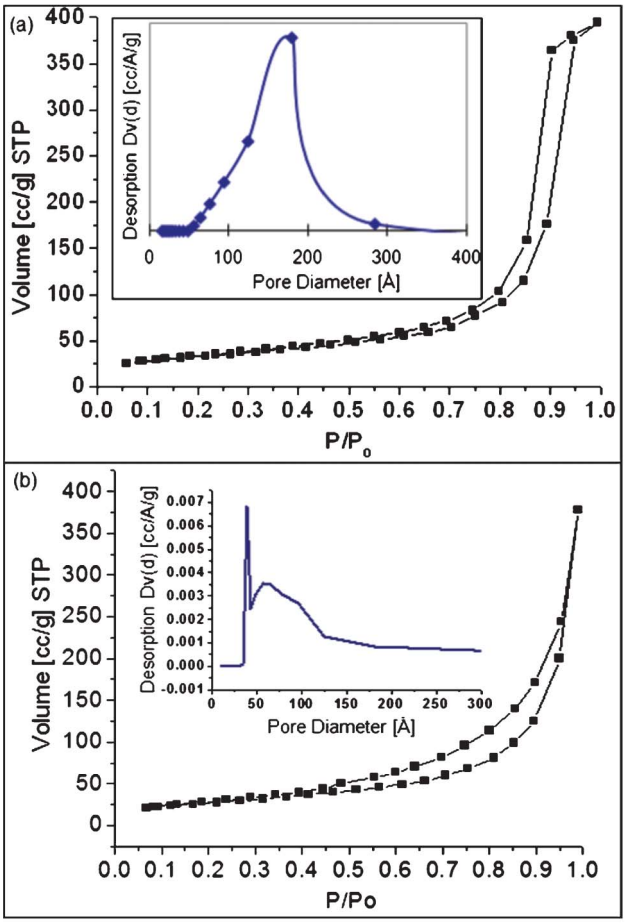

Fig. 4 BET isotherm patterns of (a) LDH (IEP) and (b) LDH (CC). The inset shows the pore size distributions.

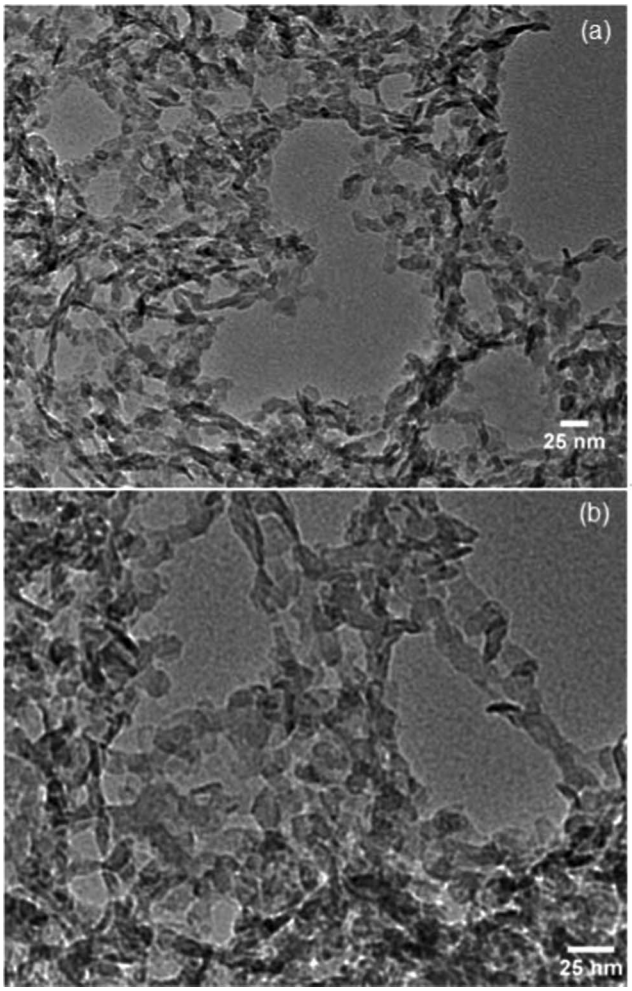

Fig. 6 (a) TEM image and (b) high-resolution TEM image of $Mg_3Al–CO_3$ LDH (IEP).

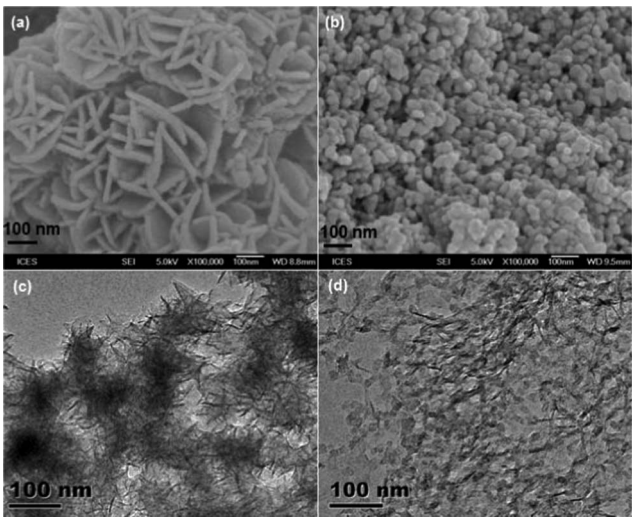

Fig. 5 SEM images of (a) LDH (CC) and (b) LDH (IEP), and TEM images of (c) LDH (CC) and (d) LDH (IEP).

''sand rose'' LDH is related to its IEP, which is around 10 for $Mg_3Al–CO_3$.[70,71] Under this condition, although the formation of the primary particles is fast, the growth is slow because the surface of the initially formed primary particles is electrically neutral (pH = IEP). Consequently, growth of the LDH particles is preferred along the 001 plane, where the surface charge density is low, resulting in a ''sand rose'' morphology.[72,73] At pH 12, although the formation of LDH was very fast under these basic conditions, its growth was inhibited. According to the IEP theory, the LDH surface is negatively charged at pH values higher than its IEP. Thus, the interaction between LDH NPs and $Al(OH)_4^-$ (and/or CO_3^{2-}, OH^-) is not favored due to repulsive forces. Consequently, LDH nano-spheres with an average diameter of 20 nm were synthesized (Fig. 6). During the washing and drying of the LDH nano-spheres, they stick together forming novel mesoporous $Mg_3Al–CO_3$ LDHs.

In order to further compare the particle size difference between LDH (CC) and LDH (IEP), DLS analysis was performed, as shown in Fig. 7. It is apparent that the sample synthesized by IEP is much smaller than that by the conventional coprecipitation method. The average DLS parti-

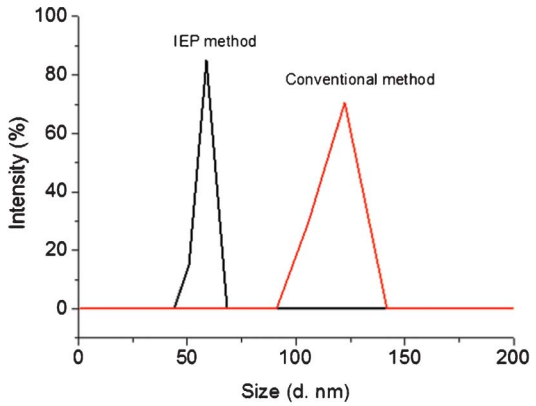

Fig. 7 Particle size distribution of Mg_3Al–CO_3 LDH (IEP) and LDH (CC) measured by DLS analysis.

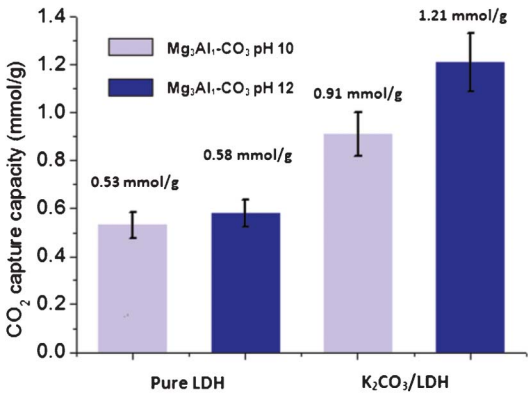

Fig. 8 CO_2 capture capacity of LDH (CC) and LDH (IEP), and 20 wt% K_2CO_3 impregnated LDH (CC) and LDH (IEP).

cle size for LDH (CC) and LDH (IEP) is 122 nm and 58 nm, respectively. It should be noted that the size difference between TEM and DLS should be attributed to the slight aggregation of LDH nanospheres in solution.[74]

3.3 CO_2 capture performance

LDHs have been widely identified as the most suitable CO_2 adsorbents in the intermediate-temperature range (200–400 °C), particularly for SEWGS. Therefore, the CO_2 capture capacity of the as-synthesized nanospherical Mg_3Al–CO_3 LDH (IEP) was compared with the traditional LDH (CC) with a ''sand rose'' morphology. A freshly prepared LDH does not possess any basic sites, however, upon thermal treatment, the LDH gradually loses interlayer water, and then dehydroxylates and decarbonates to a large extent, leading to the formation of a mixed oxide with a 3D network.[75] Ram Reddy *et al.*[49] investigated the effect of calcination temperature on a Mg–Al–CO_3 LDH and found that the sample calcined at 400 °C showed the highest CO_2 adsorption capacity. This amorphous phase has a relatively high specific surface area and exposes sufficient basic sites on the surface. Therefore, in the present work, both LDH (IEP) and LDH (CC) were first calcined at 400 °C in Ar gas for 5 h before each CO_2 adsorption test. Then the thermogravimetric sorption of CO_2 on the LDH derivatives was measured at 200 °C using a Q500 TGA analyzer, as shown in Fig. 8. It is apparent that the nanospherical LDH (IEP) has a slightly enhanced CO_2 capture capacity compared to the ''sand rose'' LDH (CC). The CO_2 capture capacity for LDH (CC) and LDH (IEP) was 0.53 and 0.58 mmol g^{-1}, respectively.

It is suggested that doping LDHs with K_2CO_3 could significantly increase its CO_2 adsorption capacity.[10,42,48,76] Walspurger *et al.*[43] investigated the K^+ promotion mechanism, and suggested that potassium ions could strongly interact with aluminium oxide centers in the LDH, resulting in the generation of basic sites that were able to reversibly adsorb CO_2 at high temperatures. In a recent report, Lee *et al.*[76] carried out a systematic study on the promoting effect of K_2CO_3 on LDHs. They found that CO_2 adsorption increased with an increase in K_2CO_3 loading, reaching a maximum adsorption capacity at *ca.* 25 wt% K_2CO_3–LDH. This result implies that an optimal K_2CO_3 loading exists for the maximum CO_2 adsorption uptake. At higher K_2CO_3 loading, the amount of CO_2 adsorption starts to decrease, which might be due to the blocking of sites within the LDH support and/or a poorer dispersion of K_2CO_3. They observed that a maximum CO_2 adsorption uptake of 0.94 mmol g^{-1} was obtained. Therefore, the promoting effect of K_2CO_3 doping on LDH (CC) and LDH (IEP) was also of great interest to us. Fig. 8 shows the CO_2 capture capacity of 20 wt% K_2CO_3–LDH (CC) and 20 wt% K_2CO_3–LDH (IEP) evaluated at 200 °C and 1 atm. After introducing K_2CO_3, K_2CO_3–LDHs were further calcined at 400 °C for 5 h before each CO_2 capture test. The result clearly indicates that K_2CO_3 doping significantly increased the CO_2 adsorption capacity, achieving 1.21 mmol g^{-1} for LDH (IEP) and 0.91 mmol g^{-1} for LDH (CC). The CO_2 adsorption capacity of the conventional K_2CO_3–LDH (CC) is comparable with the result reported by Lee *et al.*[76] However, K_2CO_3–LDH (IEP) showed a much higher CO_2 capture capacity and it is believed that the mesopores within the LDH (IEP) may favor the dispersion of K_2CO_3 and lead to its superior CO_2 capture capacity.

The application of this CO_2 adsorbent in SEWGS can be illustrated in eqn (1) and Fig. 9.

$$\text{CO (g)} + \text{H}_2\text{O (g)} + \text{adsorbent (s)} \rightarrow \text{adsorbent–CO}_2\text{ (s)} + \text{H}_2\text{ (g)} \quad (1)$$

CO_2 adsorbent is generally mixed with a WGS catalyst in the same reactor. During the CO_2 capturing process (Fig. 9(a)), the produced CO_2 will be immobilised on the surface of the solid adsorbent, resulting in the release of high purity and high-temperature H_2, which can be directly fed to gas turbines. When the adsorbent is saturated with CO_2, it can be regenerated by either temperature swing adsorption or pressure swing adsorption (Fig. 9(b)). This process can produce pure CO, which can be further converted into fuel/chemical or stored by mineralisation.[77] For the practical reaction-based CO_2 separation processes, the industrial standard is monoethanol amine (MEA), which has a CO_2 capture capacity of *ca.* 1.36 mmol g^{-1}.[78,79] The performance of our synthesised adsorbent (1.21 mmol g^{-1}) has a comparable

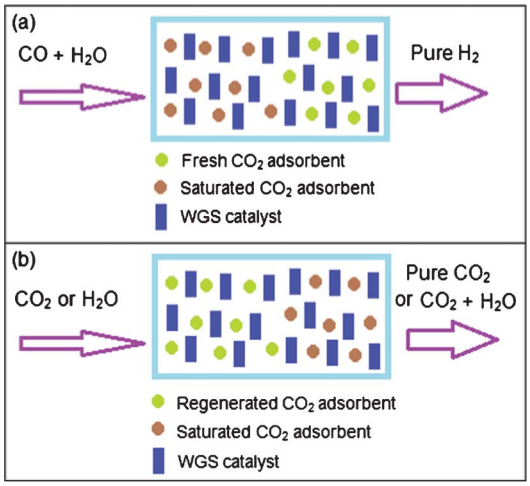

Fig. 9 SEWGS process: (a) CO_2 capturing process, and (b) CO_2 adsorbent regeneration process.

CO_2 capture capacity to an industrial standard. In addition, the synthesis method is very simple and suitable for large scale production. Regarding the economical evaluation of SEWGS, many simulations have been conducted to evaluate its application in power generation from natural gas with carbon capture.[80–82] The modelling results show that the SEWGS process could significantly reduce the cost of capturing CO_2 *versus* a reference design that uses amine absorption.[80] Manzolini *et al.*[82] reported that the removal of the CO_2 produced in the WGS reaction enhances CO conversion and thus causes a reduction in CO_2 emissions up to 95%.

4. Conclusions

In summary, we have prepared LDH nanospheres with an average size of *ca.* 20 nm using a simple method. Its unique morphology is due to fast nucleation in a high pH environment and its negative surface charge when pH > IEP. Subsequently, mesoporous Mg_3Al–CO_3 LDH, which is composed of these uniform nano-spheres, was obtained by the aggregation of the above nanoparticles. XRD analysis confirmed that LDH (IEP) forms the same layered structure as LDH (CC). In BET analysis, LDH (IEP) showed a H1 type hysteresis loop, which indicates that the pores are produced by the aggregation of uniform spheres, while LDH (CC) showed a H3 type hysteresis loop, which suggests that the pores are produced by the aggregation of the plate-like particles. SEM, TEM and DLS analyses confirmed that the particle size of LDH (IEP) is only *ca.* 20 nm, which is much lower than LDH (CC). Finally, we demonstrate that this nanospherical Mg_3Al–CO_3 LDH (IEP) has a good CO_2 capture performance. K_2CO_3–LDH (IEP) has a much higher CO_2 capture capacity (1.21 mmol g^{-1}) than K_2CO_3–LDH (CC) (0.91 mmol g^{-1}). The superior performance could be explained by its special mesoporous structure, whose big pores are favourable for the dispersion of doped K_2CO_3 species.

Acknowledgements

This work is supported by the Fundamental Research Funds for the Central Universities (YX2012-1), the Program for New Century Excellent Talents in University (NCET-12-0787), and the Key Laboratory of Functional Inorganic Material Chemistry (Heilongjiang University), Ministry of Education.

References

1 B. Balasubramanian, A. Lopez Ortiz, S. Kaytakoglu and D. P. Harrison, *Chem. Eng. Sci.*, 1999, **54**, 3543.
2 H. K. Rusten, E. Ochoa-Fernandez, H. Lindborg, D. Chen and H. A. Jakobsen, *Ind. Eng. Chem. Res.*, 2007, **46**, 8729.
3 A. L. Ortiz and D. P. Harrison, *Ind. Eng. Chem. Res.*, 2001, **40**, 5102.
4 H. T. J. Reijers, S. E. A. Valster-Schiermeier, P. D. Cobden and R. W. van den Brink, *Ind. Eng. Chem. Res.*, 2006, **45**, 2522.
5 K. B. Lee, M. G. Beaver, H. S. Caram and S. Sircar, *J. Power Sources*, 2008, **176**, 312.
6 D. P. Harrison, *Ind. Eng. Chem. Res.*, 2008, **47**, 6486.
7 P. D. Cobden, P. van Beurden, H. T. J. Reijers, G. D. Elzinga, S. C. A. Kluiters, J. W. Dijkstra, D. Jansen and R. W. van den Brink, *Int. J. Greenhouse Gas Control*, 2007, **1**, 170.
8 Q. Wang, J. Luo, Z. Zhong and A. Borgna, *Energy Environ. Sci.*, 2011, **4**, 42.
9 Q. Wang, H. H. Tay, D. J. W. Ng, L. Chen, Y. Liu, J. Chang, Z. Zhong, J. Luo and A. Borgna, *ChemSusChem*, 2010, **3**, 965.
10 Q. Wang, Z. Wu, H. H. Tay, L. Chen, Y. Liu, J. Chang, Z. Zhong, J. Luo and A. Borgna, *Catal. Today*, 2011, **164**, 198.
11 Z. Yong and A. E. Rodrigues, *Energy Convers. Manage.*, 2002, **43**, 1865.
12 S. Choi, J. H. Drese and C. W. Jones, *ChemSusChem*, 2009, **2**, 796.
13 Q. Wang and D. O'Hare, *Chem. Rev.*, 2012, **112**, 4124.
14 D. G. Evans and X. Duan, *Chem. Commun.*, 2006, 485.
15 Q. Wang, H. H. Tay, Z. Zhong, J. Luo and A. Borgna, *Energy Environ. Sci.*, 2012, **5**, 7526.
16 L. He, Y. Huang, A. Wang, X. Wang, X. Chen, J. J. Delgado and T. Zhang, *Angew. Chem., Int. Ed.*, 2012, **51**, 6191.
17 Y. Zhao, M. Wei, J. Lu, Z. L. Wang and X. Duan, *ACS Nano*, 2009, **3**, 4009.
18 J. L. Gunjakar, T. W. Kim, H. N. Kim, I. Y. Kim and S. J. Hwang, *J. Am. Chem. Soc.*, 2011, **133**, 14998.
19 C. G. Silva, Y. Bouizi, V. Fornes and H. Garcia, *J. Am. Chem. Soc.*, 2009, **131**, 13833.
20 F. Millange, R. I. Walton, L. Lei and D. O'Hare, *Chem. Mater.*, 2000, **12**, 1990.
21 I. C. Chisem and W. Jones, *J. Mater. Chem.*, 1994, **4**, 1737.
22 A. M. Fogg, J. S. Dunn, S. G. Shyu, D. R. Cary and D. O'Hare, *Chem. Mater.*, 1998, **10**, 351.
23 C. Nyambo, P. Songtipya, E. Manias, M. M. Jimenez-Gasco and C. A. Wilkie, *J. Mater. Chem.*, 2008, **18**, 4827.
24 C. Manzi-Nshuti, J. M. Hossenlopp and C. A. Wilkie, *Polym. Degrad. Stab.*, 2009, **94**, 782.
25 J. Plank, D. Zhimin, H. Keller, F. V. Hössle and W. Seidl, *Cem. Concr. Res.*, 2010, **40**, 45.

26 F. Leroux and J. P. Besse, *Chem. Mater.*, 2001, **13**, 3507.
27 Q. Wang, X. Zhang, J. Zhu, Z. Guo and D. O'Hare, *Chem. Commun.*, 2012, **48**, 7450.
28 A. C. S. Alcantara, P. Aranda, M. Darder and E. Ruiz-Hitzky, *J. Mater. Chem.*, 2010, **20**, 9495.
29 D. P. Yan, J. Lu, J. Ma, S. H. Qin, M. Wei, D. G. Evans and X. Duan, *Angew. Chem., Int. Ed.*, 2011, **50**, 7037.
30 D. P. Yan, J. Lu, J. Ma, M. Wei, D. G. Evans and X. Duan, *Angew. Chem., Int. Ed.*, 2011, **50**, 720.
31 E. Coronado, C. Marti-Gastaldo, E. Navarro-Moratalla, A. Ribera, S. J. Blundell and P. J. Baker, *Nat. Chem.*, 2010, **2**, 1031.
32 E. Coronado, J. R. Galan-Mascaros, C. Marti-Gastaldo and A. Ribera, *Chem. Mater.*, 2006, **18**, 6112.
33 Y. Lwin and F. Abdullah, *J. Therm. Anal. Calorim.*, 2009, **97**, 885.
34 X. P. Wang, J. J. Yu, J. Cheng, Z. P. Hao and Z. P. Xu, *Environ. Sci. Technol.*, 2008, **42**, 614.
35 N. D. Hutson and B. C. Attwood, *Adsorption*, 2008, **14**, 781.
36 U. Sharma, B. Tyagi and R. V. Jasra, *Ind. Eng. Chem. Res.*, 2008, **47**, 9588.
37 J. I. Yang and J. N. Kim, *Korean J. Chem. Eng.*, 2006, **23**, 77.
38 M. K. Ram Reddy, Z. P. Xu, G. Q. Lu and J. C. Diniz da Costa, *Ind. Eng. Chem. Res.*, 2008, **47**, 2630.
39 M. K. Ram Reddy, Z. P. Xu, G. Q. Lu and J. C. Diniz da Costa, *Ind. Eng. Chem. Res.*, 2008, **47**, 7357.
40 M. Dadwhal, T. W. Kim, M. Sahimi and T. T. Tsotsis, *Ind. Eng. Chem. Res.*, 2008, **47**, 6150.
41 A. D. Ebner, S. P. Reynolds and J. A. Ritter, *Ind. Eng. Chem. Res.*, 2006, **45**, 6387.
42 K. B. Lee, A. Verdooren, H. S. Caram and S. Sircar, *J. Colloid Interface Sci.*, 2007, **308**, 30.
43 S. Walspurger, L. Boels, P. D. Cobden, G. D. Elzinga, W. G. Haije and R. W. van den Brink, *ChemSusChem*, 2008, **1**, 643.
44 C. K. Krishnan, T. Hayashi and M. Ogura, *Adv. Mater.*, 2008, **20**, 2131.
45 W. Fan, M. A. Synder, K. Sandeep, S. P. Lee, C. W. Yoo, A. V. McCormick, L. R. Penn, A. Stein and M. Tsapatsis, *Nat. Mater.*, 2008, **7**, 984.
46 E. Ramasamy and J. Lee, *Energy Environ. Sci.*, 2011, **4**, 2529.
47 J. Lee, M. C. Orilall, S.C. Warren, M. Kamperman, F. J. DiSalvo and U. Wiesner, *Nat. Mater.*, 2008, **7**, 222.
48 E. L. G. Oliveira, C. A. Grande and A. E. Rodrigues, *Sep. Purif. Technol.*, 2008, **62**, 137.
49 M. K. Ram Reddy, Z. P. Xu, G. Q. Lu and J. C. D. da Costa, *Ind. Eng. Chem. Res.*, 2006, **45**, 7504.
50 L. H. Zhang, F. Li, D. G. Evans and X. Duan, *J. Mater. Sci.*, 2010, **45**, 3741.
51 A. Inayat, M. Klumpp and W. Schwieger, *Appl. Clay Sci.*, 2011, **51**, 452.
52 P. Benito, I. Guinea, F. M. Labajos and V. Rives, *J. Solid State Chem.*, 2008, **181**, 987.
53 S. P. Paredes, G. Fetter, P. Bosch and S. Bulbulian, *J. Mater. Sci.*, 2006, **41**, 3377.
54 A. Tsujimura, M. Uchida and A. Okuwaki, *J. Hazard. Mater.*, 2007, **143**, 582.
55 G. Hu, N. Wang, D. O'Hare and J. Davis, *Chem. Commun.*, 2006, 287.
56 S. Li, J. Lu, M. Wei, D. G. Evans and X. Duan, *Adv. Funct. Mater.*, 2010, **20**, 2848.
57 M. J. Climent, A. Corma, S. Iborra, K. Epping and A. Velty, *J. Catal.*, 2004, **225**, 316.
58 P. Benito, M. Herrero, F. M. Labajos and V. Rives, *Appl. Clay Sci.*, 2010, **48**, 218.
59 T. Xiao, Y. Tang, Z. Jia, D. Li, X. Hu, B. Li and L. Luo, *Nanotechnology*, 2009, **20**, 475603.
60 R. Ma, K. Takada, K. Fukuda, N. Iyi, Y. Bando and T. Sasaki, *Angew. Chem., Int. Ed.*, 2008, **47**, 86.
61 K. J. You, C. T. Chang, B. J. Liaw, C. T. Huang and Y. Z. Chen, *Appl. Catal., A*, 2009, **361**, 65–71.
62 C. T. Chang, B. J. Liaw, C. T. Huang and Y. Z. Chen, *Appl. Catal., A*, 2007, **332**, 216–224.
63 K. T. Kim, Y. G. Kim and J. S. Chung, *Carbon*, 1993, **31**, 1289–1296.
64 J. S. Choi, H. K. Youn, B. H. Kwak, Q. Wang, K. S. Yang and J. S. Chung, *Appl. Catal., B*, 2009, **91**, 210–216.
65 M. L. Toebes, J. A. van Dillen and K. P. de Jong, *J. Mol. Catal. A: Chem.*, 2001, **173**, 75–98.
66 N. Arancibia-Miranda, M. Escudey, M. Molina and M. T. García-González, *J. Non-Cryst. Solids*, 2011, **357**, 1750.
67 J. M. Kim, Y. J. Han, B. F. Chmelkab and G. D. Stucky, *Chem. Commun.*, 2000, 2437.
68 S. Cadars, G. Layrac, C. Gerardin, M. Deschamps, J. R. Yates, D. Tichit and D. Massiot, *Chem. Mater.*, 2011, **23**, 2821–2831.
69 S. Brunauer, P. H. Emmett and E. Teller, *J. Am. Chem. Soc.*, 1938, **60**, 309.
70 C. T. Chang, B. J. Liaw, C. T. Huang and Y. Z. Chen, *Appl. Catal., A*, 2007, **332**, 216.
71 K. J. You, C. T. Chang, B. J. Liaw, C. T. Huang and Y. Z. Chen, *Appl. Catal., A*, 2009, **361**, 65.
72 Y. Luo, G. Duan and G. Li, *J. Solid State Chem.*, 2007, **180**, 2149.
73 Q. L. Li, H. Lu, M. Zheng, J. Xie and Y. Chen, *J. Mater. Sci. Eng.*, 2007, **25**, 609.
74 Z. P. Xu, G. Stevenson, C.-Q. Lu and G. Q. Lu, *J. Phys. Chem. B*, 2006, **110**, 16923–16929.
75 W. Yang, Y. Kim, P. K. T. Liu, M. Sahimi and T. T. Tsotsis, *Chem. Eng. Sci.*, 2002, **57**, 2945.
76 J. M. Lee, Y. J. Min, K. B. Lee, S. G. Jeon, J. G. Na and H. J. Ryu, *Langmuir*, 2010, **26**, 18788.
77 M. Mikkelsen, M. Jørgensen and F. C. Krebs, *Energy Environ. Sci.*, 2010, **3**, 43.
78 H. Gupta and L. S. Fan, *Ind. Eng. Chem. Res.*, 2002, **41**, 4035.
79 C. T. Yavuz, B. D. Shinall, A. V. Iretskii, M. G. White, T. Golden, M. Atilhan, P. C. Ford and G. D. Stucky, *Chem. Mater.*, 2009, **21**, 3473.
80 A. Wright, V. White, J. Hufton, E. van Selow and P. Hinderink, *Energy Proc.*, 2009, **1**, 707.
81 J. D. Mondol, D. McIlveen-Wright, S. Rezvani, Y. Huang and N. Hewitt, *Fuel*, 2009, **88**, 2495.
82 G. Manzolini, E. Macchi, M. Binotti and M. Gazzani, *Int. J. Greenhouse Gas Control*, 2011, **5**, 200.

